

REFRACTORY MATERIAL SIS JUNCTION STRUCTURES

V.Yu.Belitsky, V.N.Gubankov, V.P.Koshelets, G.A.Ovsyannikov,
I.L.Serpuchenko, S.V.Shitov, M.A.Tarasov, A.N.Vystavkin
Institute of Radio Engineering and Electronics, USSR Academy of Sciences,
Marx Avenue 18, Moscow, GSP-3, 103907, USSR

Abstract

Niobium based SIS junction structures for microwave receiving devices were investigated. The possibility of the mixing efficiency improving for Nb-Al₂O₃-Nb junctions with a negative resistance near the gap voltage has been demonstrated. Comparative microwave investigation of the parallel and series DC biased arrays shows the advantage of the first one. SIS junction capacitance has been compensated with microstrip or lumped elements at the signal frequency. Such compensated structures were investigated at frequencies 38 and 76 GHz both in waveguide and quasioptic systems.

Introduction

Superconductor - Insulator - Superconductor (SIS) junctions are one of the most promising elements for low noise microwave receiving devices. SIS junctions have extremely high nonlinearity of the quasiparticle current and low intrinsic noise approaching the quantum limit. The investigations of the SIS junctions and arrays based on the soft materials have demonstrated quantum mixing with high conversion efficiency^{1,2}. Using series SIS arrays simplifies the microwave matching and expands the dynamic range of the receiver³. However, SIS junctions and arrays based on the soft materials are not rigid enough, they are subjected to aging. The aim of the present work has been an experimental investigation of the SIS mixing structure based on refractory material niobium.

Nb based SIS junctions

Earlier it has been demonstrated that Nb-Nb_xO_y-Pb+Bi junctions⁴ are suitable for quantum mixing⁵. However the specific capacitance C/A (A - junction area) of such junctions are higher than for soft material junctions; so the conversion efficiency is decreased. Therefore Nb junctions with Al interlayers⁶, having small specific capacitance and high nonlinearity of the quasiparticle IVC, have been also investigated⁷.

Nb-Al₂O₃-Nb junctions were prepared by oxidation at room temperature of the Al layer (d = 30 - 40 Å) sputtered immediately after RF etching of the bottom Nb electrode. A counter Nb electrode was deposited without vacuum breaking on the room temperature substrate; its geometry was shaped by lift off.

Prepared in this manner junctions have normal state resistance R_N = 1 - 10 Ω for areas A = 5 - 50 μm²; ratios R_J/R_N are 5 - 25, where R_J = resistance at V = 2 mV. Nb-Al₂O₃-Nb junctions remain stable at thermal cycling between helium and room temperature and two year aging.

The experimental comparison of the capacitance for two different types of the Nb based junctions is performed by determination of the resonant frequencies in specially prepared long Josephson junctions. The ratio of the specific capacitance for intrinsic Nb oxide and Al₂O₃ is estimated as 2.5 ± 0.5.

A typical IVC of the Nb-Al₂O₃-Nb junctions is shown on Fig. 1 by solid line. One can see the hysteretic "knee" at V > V_g = 2Δ/e and residual slope at V ≈ V_g. It was demonstrated in microscopic theory⁸ that proximity

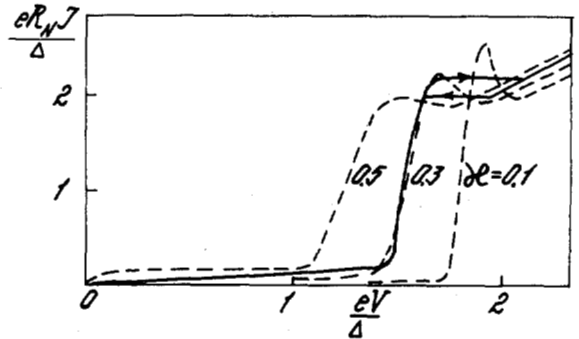


Fig. 1. IVC of Nb-Al₂O₃-Nb junction at T = 4.2 K - solid line. Dashed lines show theoretical IVCs of SNINS junction for three values of ζ (1).

effect on the boundary normal metal - superconductor in SNINS junctions leads to changing of the electron distribution function and consequently leads to residual slope at V ≈ V_g, "knee" at V > V_g, and deflection of the I_c(T) dependence from "usual" tunnel one. For quantitative analysis the parameter

$$\zeta = \frac{\sigma_N \xi_S d_N}{\sigma_S \xi_N^2} \quad (1)$$

was introduced⁸; where σ_N, σ_S = conductivity and ξ_N, ξ_S = coherence length for normal metal and superconductor correspondingly; d_N = thickness of the normal layer. Theoretical IVCs for SNINS junction with two normal layers at T/T_c = 0.6 are shown on Fig. 1 by dashed lines for different values ζ = 0.1, 0.3, 0.5. It is seen the experimental IVC conforms with theoretical one at ζ = 0.3; the same estimation for ζ is obtained from comparison with the theory² - the experimental decreasing of the V_g and I_c, the value of the hysteresis on "knee", the slope at V ≈ V_g.

For Nb-Nb_xO_y-Pb+Bi junctions the theory coincides with experiment better for one normal layer model SNIS junction at ζ = 0.1 - 0.2. It should be noted the residual slope at V ≈ V_g and "knee" for Nb-Al₂O₃-Nb junctions prepared at the same oxidation conditions by SNAP technique⁹ are reduced significantly. It indicates that the main normal layer is formed during RF cleaning of the bottom Nb electrode before Al sputtering.

Microwave properties of the Nb based junctions

The IVC peculiarities of the Nb based junctions ("knee", for example) manifest themselves in the junction microwave properties. In Fig. 2 the autonomous and pumped IVCs (f_{L0} = 72 GHz) are shown by dashed and solid line, respectively. The quantum current steps are evidently visible on the pumped curve. The variation of the IVC with local oscillator power can be explained by existence of the two independent current step sets, with distance between steps ΔV = hf_{L0}/e = 300 μV in both sets. This is caused by existence of the two regions⁷ on the autonomous IVC where sharp changing of the conductivity take place: first one in the beginning of the quasiparticle current growth at V < V_g; second - near "knee" at V > V_g.

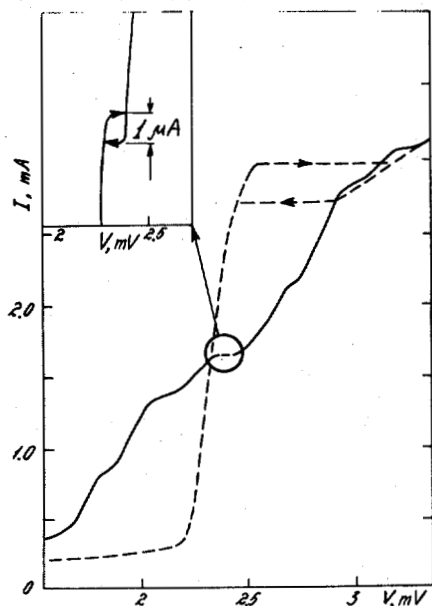


Fig. 2. Autonomous (dashed line) and pumped (solid line) IVCs of Nb-Al₂O₃-Nb junction at $f_{LO} = 72$ GHz. In the insert, the hysteretic current step is shown in detail.

In the insert of Fig. 2 the hysteretic current step is shown. The hysteresis appeared in the narrow local oscillator power range only. It is caused by hysteresis on the autonomous IVC near "knee". Existence of the region with large or negative differential resistance indicates a possibility to obtain a conversion gain greater than unity¹⁰. Therefore for Nb-Al₂O₃-Nb junctions the best conversion efficiency ($G^{max} = 0.2$) is realized at $V > V_g$.

The extremely high "knee" nonlinearity on IVC of the Nb based junctions gives the possibility to observe quantum mixing at low frequencies ($hf/e < \delta V_g; \delta V_g$ is a gap spreading).

For comparison with photon-assisted tunneling theory¹⁰ we used the Nb-Nb_xO_y-Pb+Bi junctions where $\gamma = 2\pi f C R_N$ was about 10 mm wavelength. Therefore the impedance of the junction has large imaginary part remaining nearly constant at all bias voltages and we can calculate the conversion gain $G(V, \alpha)$ ¹⁰

$$G(V, \alpha) = \left\{ \frac{\partial I(V, \alpha)}{2\alpha} \right\}^2 \frac{R_d(V, \alpha) R_{RF}(V, \alpha) 4R_d Z_0}{(hf/e)^2 (R_d + Z_0)^2}, \quad (2)$$

where

$$I(V, \alpha) = \sum_{n=-\infty}^{\infty} J_n^2(\alpha) \cdot I(V + nhf/e) \quad (3)$$

is pumped IVC, $V_{RF} = RF$ voltage, $\alpha = eV_{RF}/hf$, $I(V) =$ autonomous IVC, $R_d = dV/dI =$ the IF impedance for $f_{IF} \ll f$.

$$R_{RF}^{-1} = (2hf/e)^{-1} \sum_{n=-\infty}^{\infty} \{J_n(\alpha) + J_{n-1}(\alpha) \cdot J_{n+1}(\alpha)\} \cdot \{I(V + (n+1)hf/e) - I(V + (n-1)hf/e)\}, \quad (4)$$

where R_{RF} is impedance of the junction for signal frequency, $Z_0 = IF$ impedance of the external circuit. The theoretical conversion gain curve $G(V)$ calculated using (2) - (4) is shown on Fig. 3 (curve 3). It can be seen that there is good agreement between experiment (solid line) and theory¹⁰. Note, that for Nb-Al₂O₃-Nb junctions with smaller capacitance ($\gamma \sim 1$) it is necessary to take into account voltage dependence of the junction impedance; so it requires numerical calculations for $G(V)$.

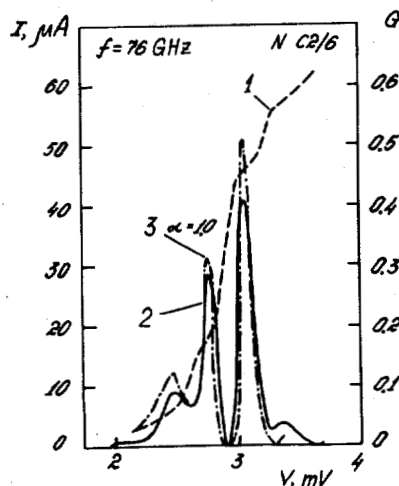


Fig. 3. Pumped IVC of Nb-Nb_xO_y-Pb+Bi junction for $f_{LO} = 76$ GHz - dashed line. Experimental conversion gain dependence $G(V)$ is shown by solid line (curve 2), calculated $G(V)$ - curve 3.

SIS junction arrays

The most important advantage of the N SIS junction arrays is the increased dynamic range as N^2 . Moreover it appears that the noise properties of an array are no worse than those in an equivalent single junction². For effective mixing the equality of the dc bias voltage on all junctions is necessary so the normal resistance tolerance should be not very large ($\Delta R_N/R_N \ll hf/eV_g$); it means the nonuniformity of the junctions should not be more than 5% for $f = 38$ GHz.

We have investigated the SIS arrays with dc parallel biasing of the junctions⁴ (See Fig. 4). All thirteen junctions in the array are connected by superconductor inductive loops ($L = 10^{-9} - 10^{-8} H$) which provides the equal dc biasing voltage on the junctions. This loop represents a large RF impedance, therefore RF currents flow directly through SIS junctions. Junction nonuniformity results in variation in the LO power only. For low intermediate frequencies, the junctions are connected in parallel; the equivalent circuit for the IF signal is shown on Fig. 5. Using equations (2) - (4) and the equivalent circuit (Fig. 5) it is possible to obtain the expression for the conversion gain of the ar-

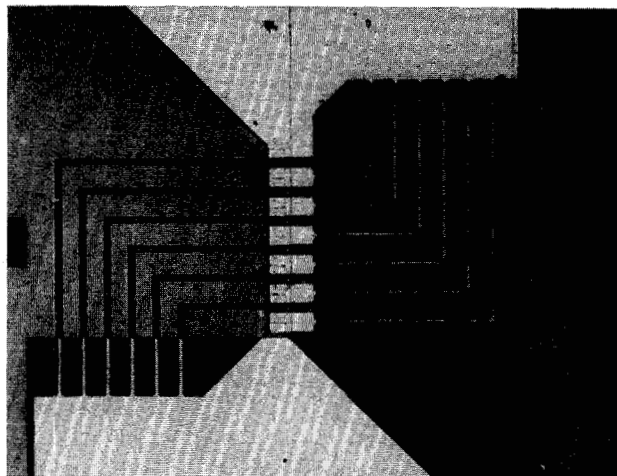


Fig. 4. Photograph of 13 junctions array with parallel dc biasing.

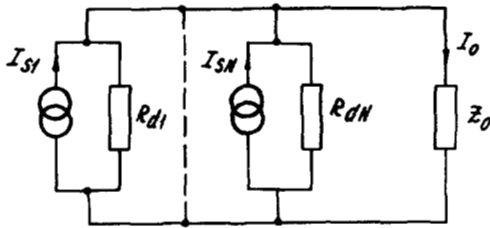


Fig. 5. Equivalent circuit of N-junction array.

$$G(V, \alpha) = \left\{ \sum_{i=1}^N \frac{\partial I_i}{2\alpha} \right\}^2 \cdot \frac{Z_O}{(hf/e) \left(1 + \sum_{i=1}^N \frac{Z_O}{R_{d_i}} \right) \cdot \sum_{i=1}^N \frac{1}{R_{RF_i}}} \quad (5)$$

For uniform spread of the junction normal resistances in the array and at $R_N^{max}/R_N^{min} = 2$ the estimation from (5) shows that conversion gain of the array with parallel biasing is decreased by 3 dB only. It is much better than for usual series array with the same non-uniformity.

Thus SIS arrays with parallel dc biasing allow at the same time:

- i) Increase the tolerance for junction nonuniformity;
- ii) Provide matching at the signal frequency of the source and RF-array impedance $R_{RF}^{ar} \approx NR_N (2hf/eV_g)$;
- iii) Provide the matching at the IF frequency of the output-array impedance and input-IF-amplifier resistance. So, parallel arrays give us the possibility to optimize the RF and IF matching simultaneously by choosing number of junctions N. If we know Z_S and Z_O we can calculate the optimal value N:

$$Z_S/Z_O = R_{RF}^{ar}/R_{IF}^{ar} = N^2 (R_N/R_d) 2hf/eV_g = N^2 \cdot const. \quad (6)$$

For comparison different types of arrays we have investigated experimentally single junction, parallel, and series dc-biased arrays fabricated on the same substrate. The junctions have areas about $60 \mu m^2$. The reduced sensitivity for both type of arrays differ less than 1 dB in spite of the difference of the normal state resistance for $N^2 = 169$. Thus the dc-bias inductive circuits provide efficient isolation for RF current. Quantum mixing has been obtained for single junctions and both types of the arrays at $f = 38$ GHz, but conversion photon peaks for series arrays were smaller than ones for parallel arrays and single junctions. Saturation measurements were performed by IF photon peak reduction. Normalized quantum conversion efficiency vs normalized signal power for a single junction and both type of the arrays is shown in Fig. 6. Signal power is normalized

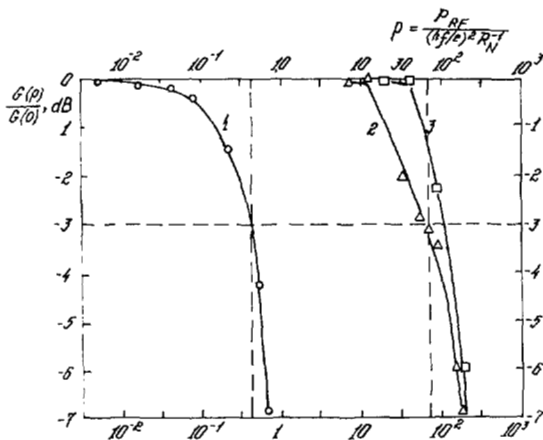


Fig. 6. Normalized conversion efficiency vs signal power for three types of the SIS structures: o - single junction; Δ - array with dc parallel biasing; \square - series array.

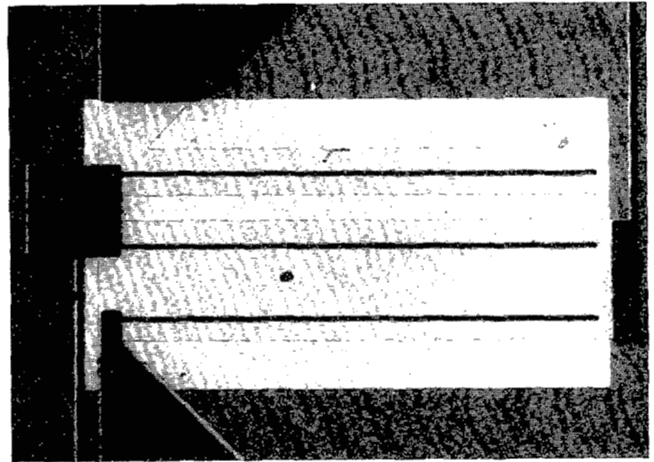


Fig. 7. Three-junction parallel dc-biased array with open-circuit microstrip stubs.

to $(hf/e)^2/R_N$ which is approximately equal to the IF output saturation power for single junction. Fig. 6 shows that 3 dB reduction of the conversion gain takes place at the same input signal power level for both array types. This level is N^2 times more than for single junction that agrees with data for series arrays².

Junction capacitance tuning out.

The large junction capacitance effectively shunts the mixer at harmonic frequencies but must be tuned out at the signal frequency. This is usually accomplished by an elaborate matching circuit which leads to narrow bandwidth¹¹ and reduction of the junction real part impedance $1/(1 + \gamma^2)$ ¹². For optimal junction capacitance ($1 < \gamma < 10$) this reduction is significant. Optimization of SIS mixer requires tuning element external to the junction but close enough to minimize losses in signal circuits¹¹⁻¹³.

We have investigated two types of junction capacitance tuning-out circuit. Fig. 7 shows three-junction array with open-circuited superconducting microstrip stubs (length $l_s > \lambda/4$) which act as a parallel inductance across the junctions^{11,13}. The data shows that the microstrips in our case are perpendicular to current flow and can be applied to mixer blocks with reduced-height waveguide. Counter Pb+Bi microstrip electrode (width $w = 10 \mu m$) is separated from bottom Nb one by SiO layer ($d = 3000 - 4500 \text{ \AA}$). The soft material of the counter electrode provides the possibility of resonant frequency tuning by changing of the stub length. Fig. 8 shows the detector response ratio for junctions with and without capacitance tuning out at two different stub lengths. The solid curves show the theoretical ones calculated for case $Z_S \gg R_{RF} = const$:

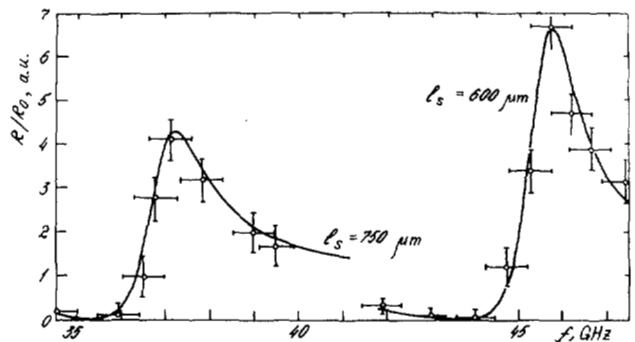


Fig. 8. Detector response frequency dependence of the junction with tuning out capacitance by open-circuited microstrip stub for two lengths $l_1 = 600 \mu m$ and $l_2 = 750 \mu m$.

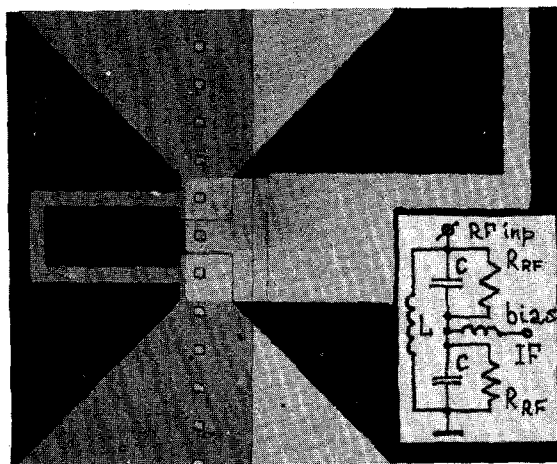


Fig.9. Photography of a two-junction cell with superconducting inductive loop for tuning out of the capacitance. The equivalent circuit of the cell is shown in insert.

$$R/R_0 = |Z|^2 \cdot (1 + \gamma^2) / R_{RF}^2, \quad (7)$$

$$|Z|^2 = \left\{ (1/R_{RF})^2 + [2\pi f C + 1/\rho \cdot \text{tg}(\beta l_s)]^2 \right\}^{-1},$$

where Z = stub and junction parallel circuit impedance, ρ = characteristic impedance of the microstrip line, $\beta = 2\pi/\lambda_0$ = propagation constant¹⁴. The resonance curve shape provides a convenient method for determination of the system parameters. For example, at frequency where $l_s = \lambda/4$, there is shunting of the junction impedance and response is decreased to zero. For data represented on Fig. 8 the best fitting takes place at $\rho = 8\Omega$, $C = 6\text{pF}$, $R_{RF} = 1.4\Omega$, $\sqrt{\epsilon} = 3.9$, agreeing well with another estimation of these parameters.

In the second case we have investigated the tuning out of the junction capacitance by lump inductance provided at the same time dc parallel biasing of the junctions in array. Fig. 9 shows the cell of two SIS junctions with inductance loop ($L = 2 \cdot 10^{-10}\text{H}$ is selected to resonate junction capacitance at signal frequency). Such cells are most suitable for using in parallel dc biasing arrays.

Planar quasi-optical mixer

In recent years an increased interest in application of quasi-optical mixers and detectors at mm wavelength has been observed¹⁵⁻¹⁷. The advantages of such devices are very wide bandwidth without any additional tuning and avoidance of the polarization losses. These advantages of the quasi-optical devices become more

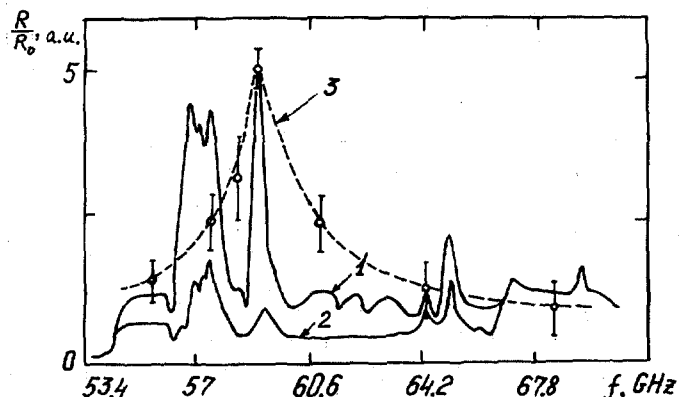


Fig. 10. Detector response frequency dependence of the junction with capacitance tuning out by inductive loop (curve 1) and without tuning (curve 2). Curve 3 - ratio of the responses with and without tuning.

important at the short mm wavelengths.

A receiving structure combining SIS junctions with tuning out circuit and planar antenna has been elaborated. The capacitance tuning out of Nb-Nb₂O₃-Pb+Bi junction is provided by thin film superconducting loop with width 20 μm and area 1000 μm^2 . For dc biasing, the capacitance ($C = 0.3\text{pF}$) is formed in the loop. The receiving structure is arranged across circular waveguide (diameter 16 mm) for RF signal (50 - 70GHz). The special absorber installed around the sample provides nondistorted microwave field in vicinity of the junction; so we can estimate input substrate power by measuring power in oversized waveguide. Absorbed RF SIS junction power is determined by measuring the first quasiparticle step oscillation. The antenna losses of input signal power is $6 \pm 3\text{dB}$, taking into account antenna ($R_{\text{ant}} = 70\Omega$) and RF SIS junction ($R_N = 20\Omega$) mismatching.

We also have investigated the influence of tuning out element in this structure. Fig. 10 shows the detector response frequency dependence of the structure with (curve 1) and without (curve 2) tuning out element. Nonmonotonic frequency dependence is caused by external electrodynamic system. Ratio of curve 1 and 2 gives the advantage (curve 3) caused by the tuning out element.

References

1. W.R. McGrath, P.L. Richards, H.D. Smith, H. Van Kempen, R.A. Batchelor, D.E. Prober, R. Santhnam, *Appl. Phys. Lett.* 39, 655, 1981.
2. W.R. McGrath, A.V. Raisanen, P.L. Richards, *IEEE Tr. on Magnetics MAG-21*, 212, 1985.
3. M.J. Feldman, S.K. Pan, A.R. Kerr, A. Davidson, *IEEE Tr. on Magnetics MAG-19*, 494, 1983.
4. A.N. Vystavkin, V.N. Gubankov, K.I. Konstantinyan, V.P. Koshelets, Yu.V. Obukhov, *Physica B+C*, 109+110, 2064, 1982.
5. V.N. Gubankov, K.I. Konstantinyan, V.P. Koshelets, G.A. Ovsyannikov, A.N. Vystavkin, *IEEE Tr. on Magnetics MAG-19*, 968, 1983.
6. M. Gurwitch, M.A. Washington, H.A. Huggins, J.M. Rowell, *IEEE Tr. on Magnetics MAG-19*, 791, 1983.
7. A.N. Vystavkin, V.P. Koshelets, G.A. Ovsyannikov, I.L. Serpuchenko, S.V. Shitov, *Sov. J. of Techn. Phys. Lett.* 11, 290, 1985 (in Russian).
8. A.A. Golybov, M.Yu. Kupriyanov, V.F. Lukichev, *Sov. J. of Low Temp. Phys.* 10, 789, 1984 (in Russian).
9. H. Kroger, L.N. Smith, D.W. Jillic, *Appl. Phys. Lett.* 39, 280, 1981.
10. J.R. Tucker, M.J. Feldman, *Reviews of Modern Physics*, 57, 1055, 1985.
11. L.R. D'Addario, *Inter. J. of Infrared and Millimeter Waves* 5, 1419, 1984.
12. V.Yu. Belitsky, V.P. Koshelets, G.A. Ovsyannikov, S.V. Shitov, "Microwave detector", a.c. N1270869, 1985.
13. A.V. Raisanen, W.R. McGrath, P.L. Richards, F.L. Lloyd, *IEEE Tr. MTTT-33*, 1495, 1985.
14. T.R. Cheewala, *IBM J. Res. and Dev.* 24, 130, 1980.
15. S. Rudner, M.J. Feldman, E. Kollberg, T. Claeson, *IEEE Tr. on Magnetics MAG-17*, 690, 1981.
16. K.E. Irwin, T. Van Duzer, S.E. Schwarz, *IEEE Tr. on Magnetics MAG-21*, 216, 1985.
17. M.J. Wengler, D.P. Woody, R.E. Miller, T.G. Phillips, *Int. J. of Infrared and Millimeter Waves* 6, 697, 1985.